$$\frac{\partial S_{se}}{\partial t} = FK_D \frac{\partial C}{\partial t} \tag{16.53}$$

The adsorption rate for type 2 kinetic nonequilibrium sites can be given by a linear and reversible first order equation of following form

$$\frac{\partial S_{sk}}{\partial t} = \alpha[(1 - F)K_D C - S_{sk}] \tag{16.54}$$

where α is the first order rate coefficient. Combining above equations with Eq. (16.14) lead to following formulation (van Genuchten, 1981; Nkedi-Kizza et al., 1984):

$$\left(1 + \frac{F\rho_b K_D}{\theta}\right)\frac{\partial C}{\partial t} + \frac{\rho_b}{\theta}\frac{\partial S_{sk}}{\partial t} = D\frac{\partial^2 C}{\partial x^2} - v\frac{\partial C}{\partial x} \tag{16.55}$$

$$\frac{\partial S_{sk}}{\partial t} = \alpha[(1 - F)K_D C - S_{sk}] \tag{16.56}$$

16.16 INITIAL AND BOUNDARY CONDITIONS FOR STEP INPUT EXPERIMENTS

The analytical solutions of Eqs. (16.23), (16.24), (16.25), (16.43), (16.44), (16.48), (16.49), (16.55), and (16.56) are available for a large number of initial and boundary conditions for both finite and semi-infinite systems for both step and pulse type solute application (van Genuchten 1981, van Genuchten and Alves, 1982). This section briefly describes some of the initial and boundary conditions required for solving solute transport equations. The most common initial condition for any soil is:

$C(x, 0)=C_i$ (16.57)

At the upper boundary of the soil surface or (or inflow into the soil column; i.e. at $x=0$), two different boundary conditions can be considered. The first type or constant concentration boundary condition is of the form as follows:

$C(0, t)=C_0$ (16.58)

For column displacement experiments, where chemical is applied at a constant rate, the boundary condition (16.58) leads to mass balance errors, which become quite significant for large values of *(D/v)* (van Genuchten, 1981, Parker and van Genuchten, 1984). The other boundary condition is a third type, or constant flux type, that leads to the conservation of mass inside the soil column provided dispersion outside the soil can be ignored is given as follows:

$$\left[-D\frac{\partial C}{\partial x}+vC\right]|_{x=0}=vC_0 \tag{16.59}$$

A third type inlet condition is usually preferred over first type inlet condition (van Genuchten and Parker, 1984, Toride et al., 1993). In order to describe the outlet conditions, it is assumed that the concentration is macroscopically continuous at the outlet and no dispersion occurs outside the soil. Parker and van Genuchten, (1984) suggested that by assuming that the upstream solute concentrations are not affected by the outlet boundary, solutions for an infinite outlet condition can be applied to the finite region. The outlet condition for a semi infinite profile ($0\leq x<\infty$) and a finite system of length L can be specified in terms of zero concentration gradient as below

$$\left(\frac{\partial C}{\partial x}\right)(\infty,t)=0 \tag{16.60}$$

$$\left(\frac{\partial C}{\partial x}\right)(L,t)=0 \tag{16.61}$$

The boundary condition [Eq. (16.60)] assumes a semi-infinite soil column and is commonly used. When effluent curves from finite columns are calculated using analytical solutions based on boundary condition [Eq. (16.60)], some errors may be introduced. Therefore, zero concentration gradient at the upper end of the column as specified by Eq. (16.61) is frequently used for column displacement studies. However, there is no evidence available to prove that the boundary condition Eq. (16.61) leads to a better description of physical processes at and around $x=L$. On the other hand, the boundary condition [Eq. (16.59)] gives a discontinuous distribution at the inlet, which is against the requirement of a continuous distribution at $x=L$ (van Genuchten, 1981).

16.17 DIMENSIONAL INITIAL AND BOUNDARY CONDITIONS FOR PULSE APPLICATION

Assuming that the concentrations are continuous across the inlet boundary and that input solution is well mixed, a first type boundary condition across the inlet boundary for a pulse type injection can be specified as (van Genuchten, 1981):

$C(0, t)=C_0\ 0<t<t_0$

$C(0, t)=0 t>t_0$ (16.62)

A third type boundary condition for the pulse input for a well mixed input solution can be specified as

$[-D(\partial C/\partial x)+vC]|_{x=0}=vC_0\ 0<t\leq t_0$

$[-D(\partial C/\partial x)+vC]|_{x=0}=0\ t>t_0$ (16.63)

The two-site model [Eqs. (16.55) and (16.56)] can be solved for the boundary and initial conditions given by Eqs. 16.57 to 16.61. One additional initial condition for the solution is

$$S_{sk}(x, 0)=(1-F)K_D C_i \tag{16.64}$$

The initial condition and the boundary conditions at exit remain the same as described by Eqs. (16.52), (16.55), and (16.56). The boundary condition at inlet, Eq. (16.57), becomes inappropriate when the input solution is not well mixed. Other arguments against the applicability of Eq. (16.57) can be that the plane considered as a macroscopic boundary has no physical relevance at the microscopic level, as irregularity in pore structure and morphology become manifest at this level. Also the medium properties vary continuously over a finite transition zone of $l/2$, where l is the representative elementary volume (REV) of the porous medium (Parker and van Genuchten, 1984).

16.18 THE COMBINED NONDIMENSIONAL TRANSPORT EQUATIONS

Nonequilibrium transport Eqs. (16.31), (16.32), (16.36), (16.37), (16.43), and (16.44) are mathematically equivalent and transferring nondimensional quantities listed in Table 16.4 reduces them to the following combined nondimensional equations (van Genuchten, 1981; Nkedi-Kizza, 1984)

$$\beta R\frac{\partial C_1}{\partial T}+(1-\beta)R\frac{\partial C_2}{\partial T}=\frac{1}{P}\frac{\partial^2 C_1}{\partial Z^2}-\frac{\partial C_1}{\partial Z} \tag{16.65}$$

$$(1-\beta)R\frac{\partial C_2}{\partial T}=\omega(C_1-C_2) \tag{16.66}$$

where β is partition coefficient, ω is nondimensional mass transfer parameter and P is peclet number. Initial and boundary conditions for a step type input are

$$C_1(x, 0)=C_2(x, 0)=0 \tag{16.67}$$

$$-\frac{1}{P}\frac{\partial C_1}{\partial x}+C_1|_{x=0}=1 \tag{16.68}$$

$$\frac{\partial C_1}{\partial x}(\infty, T)=\frac{\partial C_2}{\partial x}(\infty, T)=0 \tag{16.69}$$

For β=1, Eqs. (16.65) and (16.66) reduce to the nondimensional CDE. Some of the analytical solutions of Eqs. (16.17), (16.65), and (16.66) are given in Table 16.5.

16.19 ESTIMATION OF SOLUTE TRANSPORT PARAMETERS

The equilibrium solute transport equation [refer to Eq. (16.17)] has two parameters: (i) the apparent diffusion coefficient *(D)* or *P (vL/D)* and (ii) the retardation factor *(R).*

TABLE 16.4 Nondimensional Variables Introduced in the Solute Transport Equations

The nondimesional variables				
FOR ALL THE EQUATIONS				
$T=\frac{vt}{L}$	$Z=\frac{x}{L}$	$P=\frac{vL}{D}$	$R=1+\frac{\rho K_D}{\theta}$	$C_1=\frac{C-C_i}{C_0-C_i}$
FOR TWO REGION EQUATION				
$R_m=1+\frac{F\rho K_D}{\theta_m}$	$\beta=\frac{\theta+F\rho K_D}{\theta+\rho K_D}=\frac{R_m}{R}$	$\omega=\frac{\alpha_2(1-\beta)RL}{v}$	$C_2=\frac{S_{s2}-(1-F)K_DC_i}{(1-F)K_D(C_0-C_i)}$	
FOR TWO REGION EQUATION				
$C_1=C_m/C_0$	$C_2=C_m/C_0$	$P=\frac{v_mL}{D_m}$	$\phi_m=\frac{\theta_m}{\theta}$	$\omega=\frac{\alpha L}{q}$
$R_m=1+\frac{f\rho K_D}{\theta_m}$	$R_{im}=1+\frac{(1-f)\rho K_D}{\theta_{im}}$		$\beta=\frac{\theta_m+f\rho_bK_D}{\theta+\rho_bK_D}=\frac{\phi_mR_m}{R}$	
$C_1=\frac{C_m-C_i}{C_0-C_i}$	$C_2=\frac{C_{im}-C_i}{C_0-C_i}$	$T=\frac{v_m\phi_mt}{L}$		$q=\theta_mv_m$

Source: Modified from van Genuchten, 1981.

TABLE 16.5 Analytical Solutions of Equilibrium CDE and Nonequilibrium (NE) Transport Equations

sionless	Concentration-type boundary conditions		Flux-type boundary conditions	
tration	$C_1(0, T)=1$	$\frac{\partial C_1(\infty, T)}{\partial Z}=0$	$\left(-\frac{1}{P}\frac{\partial C_1(Z, T)}{\partial Z}+C_1(Z, T)\right)\Big\|_{z=0}=1$	$\frac{\partial C_1(\infty,$
	$C_e=\frac{1}{2}\text{erfc}\left[\left(\frac{P}{4RT}\right)^{1/2}\cdot(R-T)\right]+\frac{1}{2}\exp(P)\cdot\text{erfc}\left[\left(\frac{P}{4RT}\right)^{1/2}\cdot(R+T)\right]$		$C_e=\frac{1}{2}\text{erfc}\left[\left(\frac{P}{4RT}\right)^{1/2}\cdot(R-T)\right]+\left(\frac{PT}{\pi R}\right)^{1/2}\cdot\exp\left[-\frac{P}{4RT}\cdot(R-T)^2\right]-\frac{1}{2}\cdot\left(1+P+\frac{PT}{R}\right)\cdot\exp(P)\cdot\text{erfc}\left[\left(\frac{P}{4RT}\right)^{1/2}\cdot(R+T)\right]$	

dels	$G(\tau) = \frac{1}{2}\operatorname{erfc}\left[\left(\frac{P}{4\beta R\tau}\right)^{1/2}\cdot(\beta R-\tau)\right] + \frac{1}{2}\exp(P)\cdot\operatorname{erfc}\left[\left(\frac{P}{4\beta R\tau}\right)^{1/2}\cdot(\beta R-\tau)\right]$	$G(\tau) = \frac{1}{2}\operatorname{erfc}\left[\left(\frac{P}{4\beta R\tau}\right)^{1/2}\cdot(\beta R-\tau)\right] + \left(\frac{P\tau}{\pi\beta R}\right)^{1/2}\cdot\exp\left[-\frac{P}{4\beta R\tau}\cdot(\beta R+\tau)^2\right] - \frac{1}{2}\cdot\left(1+P+\frac{P\tau}{\beta R}\right) \cdot\exp(P)\cdot\operatorname{erfc}\left[\left(\frac{P}{4\beta R\tau}\right)^{1/2}\cdot(\beta R+\tau)\right]$
	$F(\tau) = \frac{\beta}{\tau}\left(\frac{PR}{4\pi\beta\tau}\right)^{1/2}\cdot\exp\left[-\frac{P}{4\beta R\tau}\cdot(\beta R-\tau)^2\right]$	$F(\tau) = \left(\frac{P}{\pi\beta R\tau}\right)^{1/2}\cdot\exp\left[-\frac{P}{4\beta R\tau}\cdot(\beta R-\tau)^2\right] - \frac{P}{2\beta R}\cdot\exp(P)\cdot\operatorname{erfc}\left[\left(\frac{P}{4\beta R\tau}\right)^{1/2}\cdot(\beta R+$

rce: Modified from van Genuchten, 1981.

16.19.1 Retardation Factor *(R)*

From Measured Breakthrough Curve

The retardation factor *(R)* can be estimated by locating the number of pore volumes *(T=R)* at which the relative concentration of the measured ETC is 0.5. For the measured chloride ETC in Fig. 16.8, the value of *T* at C/C_0 of 0.5 is 1.2. Therefore, the value of *R* is also 1.2. Both pore volumes *(T)* and retardation factor *(R)* are dimensionless.

From Batch Experiment

The batch experiments for solute adsorption are performed by mixing air-dried soil and solution (1:1). At least six different initial solution concentrations, which are within the experimental range, are usually selected. Generally three to four replications for each concentration are made. The mixture is stirred, and after equilibrating for 24 hours, is centrifuged and the concentration of the extracted solution is measured. The difference between the initial solution concentration and that in the supernatant (centrifuge) is assumed to be the result of adsorption. A graph is plotted between the solution concentration and the adsorbed concentration (Fig. 16.6) and the slope of the line gives the value of distribution coefficient *(K_D)* The R can be calculated from Eq. (16.18) for known values of bulk density and water content of soil in the experiment.

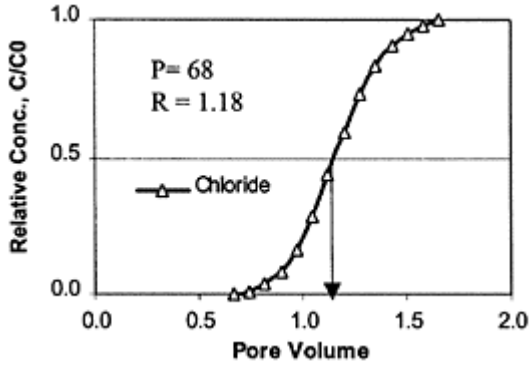

FIGURE 16.8 The estimation of retardation coefficient from a measured ETC ($R=T=1.2$) where T is pore volumes. (Redrawn from Shukla and Kammerer, 1998.)

By Fitting Flow Velocity

The pore water velocity can be used as a fitting parameter in the trial and error method while keeping R a constant and equal to 1. Therefore, fitted velocity will effectively be a v/R value. The slope of the plot between fitted and measured pore water velocity gives an effective R-value.

From Travel Time Analysis

Time moment analysis provides a model independent tool for characterizing the solute BTCs. The first temporal moment provides the mean break-through time, the second central temporal moment (i.e., the variance) describes the solute spreading, and the third (skewness) describes the degree of asymmetry of the BTCs (Valocchi, 1985). These numerical estimates can be compared to the CDE theoretical travel time moments to provide estimates of the CDE model parameters, in contrast to least-squares fitting of the analytical solution to Eqs. (16.23) and (16.24). For a finite pulse, the expected or theoretical mean travel time to depth L is:

$$\frac{RL}{v}+\frac{t_0}{2} \tag{16.70}$$

and the theoretical travel time variance is

$$\frac{2DR^2L}{v^3}+\frac{(t_0)^2}{12} \tag{16.71}$$

where R is retardation factor, D is apparent dispersion coefficient (cm^2h^{-1}), v is pore water velocity (cmh^{-1}), t_0 is the duration of pulse (h), and L is the displacement length (cm). For the step input experiments, a smooth cubic spline to each BTC can be fitted, and then the derivatives can be computed with respect to time. The center of mass of an inert solute pulse under steady flow at a given average measured pore water velocity *(v)* is model independent and moves at the same rate as the average *v*. However, different process models often result in quite different rates of spreading or dispersion but these do not affect the mean travel time (Valocchi, 1985). The slope of the best-fit curve between observed and theoretical travel times provides the effective R-value with intercept equal to zero. For details on travel moment analysis readers are advised to refer Jury and Roth (1990).

16.19.2 Apparent Dispersion Coefficient

The apparent dispersion coefficient (D) can be estimated by the following methods.

Trial and Error Method

The parameters D (or P) can be estimated by comparing the experimentally measured ETC with a series of calculated distributions. The distributions can be calculated for a known value of R *(=T)* by selecting several values of P (1, 2, 4, 5, 10, 20, 50, 100, 300, etc.). The value of P, which provides the best fit between the experimental and calculated BTC is chosen, and D is calculated from the known values of displacement length and pore water velocity *(D=vL/P)*.

From Slope of an Effluent Curve

The apparent diffusion coefficient can be approximated by an experimental BTC from the following equation (Kirkham and Powers, 1972)

$$D = \frac{vL}{4\pi m^2} \tag{16.72}$$

where m is the slope of BTC at one pore volume, i.e.,

$$m = \frac{\partial(C/C_0)}{\partial p}\Big|_{p=1}. \tag{16.73}$$

Log Normal Plot of Effluent Curve

In this method the inverse complimentary error function of relative concentration (see Table 16.5) from the experimentally determined BTC is plotted against log of pore volumes *(T)*. The value of P is estimated from the slope *(m)* of above straight line ($P=4*m^2-b$, where b is a correction factor) (van Genuchten and Wierenga, 1986).

Least Square Analysis

The trail and error method is expanded into a more rigorous approach by continuously adjusting the values of P and R until the sum of the

TABLE 16.6 Merits and Demerits of Approximate Methods of Solute Transport Parameter Estimation

Method	Merits	Demerits
Trial and error	Provide first estimates of *P* and *R* quickly	Method is not necessarily reproducible
From slope of ETC	Method is simple and based upon analytical solution. For conservative solutes works reasonably well.	Method is not suitable for small values of *P* and for nonconservative solutes
Log normal plot	Results are more accurate than the above two methods	Straight line is not generally obtained. Method is not suitable for aggregated or structured soils
Least square analysis	Results are the most accurate among all the methods described above. Computer programs are available and easy to use. Number of fitting parameters can be varied according to the need	User judgment is necessary for reporting fitted values of parameters

squared deviations between measured and fitted concentrations are minimized in a least square sense (van Genuchten and Wierenga, 1986). The merits and demerits of all the methods described above are presented in Table 16.6.

16.19.3 Parameters of TRM

The physical nonequilibrium model or two-region model (TRM) requires specification of four dimensionless parameters P (v_m, L, D), R(ρ_b, K_D, θ), β ($\phi, \theta_m, \theta_{im}, f$) and ω (α, L, θ_m, v_m) [refer Eqs. (16.65) and (16.66)]. The parameters of TRM can be estimated by a number of ways:

Least Square Fitting

The first option is to use a trial-and-error method and fit all the four-nondimesional parameters to the measured breakthrough curve, also known as "inverse modeling technique," by minimizing the sum of squares between measured and fitted breakthrough curves using a nonlinear least square method. The second option is to determine R from the batch experiment and obtain the remaining three-nondimensional parameters by least square fit. It should be remembered while using the least square method that for P values >5, the least square fitting method is appropriate, however for P<5, the problems associated with conservation of mass become important and trial and error method remains no longer appropriate. The lower P values also suggest extremely broad range in pore water velocity distributions in mobile water region, which renders division of flow

domain into two flow regions inadequate. A possible solution is to divide flow domain in more compartments (Morisawa et al., 1986) or consider pore water velocity to be a continuous function (White et al., 1986).

Mobile (θ_m) and Immobile (θ_{im}) Water Contents

The total moisture content (θ) of the soil is the sum of the mobile (θ_m) and immobile (θ_{im}) moisture contents. The mobile and immobile water can be estimated in a number of ways: (i) all the water held at field capacity (24 h after the infiltration test or at suction of 330 kPa) can be considered as immobile water. Therefore, mobile water (θ_m) can be obtained by subtraction the θ_{im} from total water content of soil (θ) as follows:

$$\theta_m=\theta-\theta_{im} \tag{16.74}$$

(ii) The total concentration in soil after infiltration test is given by a mass balance equation as follows:

$$\theta C=\theta_m C_m+\theta_{im} C_{im} \tag{16.75}$$

A conservative tracer such as bromide (Br) or chloride (Cl) of known initial concentration (C_0) used as a solute is infiltrated into the soil. After the steady state infiltration with tracer solution is achieved, the concentration of the solute extracted from soil sample (C) below the infiltration can be measured. If all the soil moisture is mobile than C equals C_0. If immobile moisture is present $C<C_0$ and θ_{im} can be obtained as follows (Clothier, et al., 1992):

$$\theta_m = \theta\frac{C}{C_m} = \theta\frac{C}{C_0} \tag{16.76}$$

alternately

$$\theta_{im} = \theta\left(1-\frac{C}{C_0}\right) \tag{16.77}$$

The above equation assumes that transfer coefficient (α) in Eq. (16.56) is small and very little solute diffuses into the immobile region.

The θ_{im} and α

The θ_{im} and α can also be estimated simultaneously by applying a sequence of nonconservative nonreactive tracers for varying periods of time (Jaynes et al., 1995).

Eq. (16.37) after separating the variables can be written as follows:

$$\ln\left(1-\frac{C}{C_0}\right) = \frac{-\alpha}{\theta_{im}}t + \ln\left(\frac{\theta_{im}}{\theta}\right) \tag{16.78}$$

where t is defined as the application time and varies for different tracers, Plotting the $ln(1-C/C_0)$ versus t, for all the tracers, gives straight lines with negative slopes (Fig. 16.9). The intercept at t=0 gives natural log of the

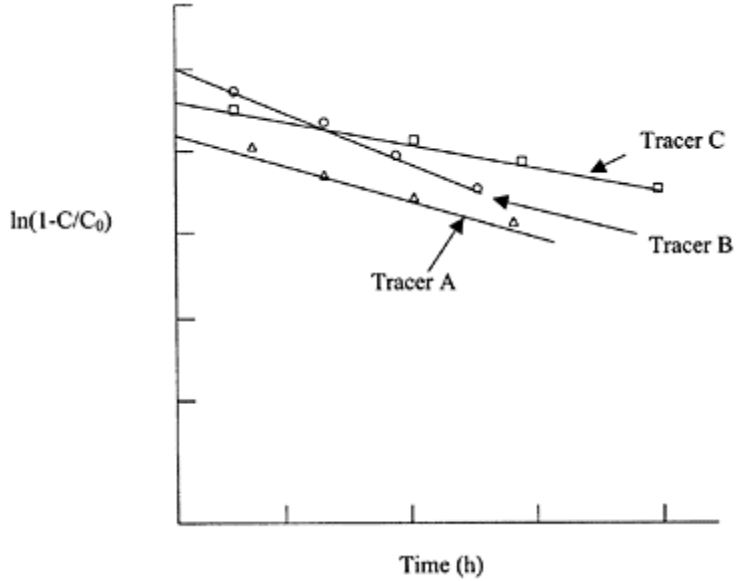

FIGURE 16.9 A schematic of normalized concentration of tracers and the time of application.

ratio of immobile water and total moisture content [the second term on right-hand side of Eq. (16.78)]. For a known θ, θ_{im} can be estimated by multiplying the intercept with θ and making appropriate In transformations. The first term of Eq. (16.78) gives the slope and for a known θ_{im}, a can be easily calculated. The tracer front will reach a given sampling depth *(d)* slightly earlier than specified by *t.* Therefore, t in Eq. (16.78) can be replaced by "t-d/v_m" and Eq. (16.77) becomes (Jaynes and Horton, 1998):

$$\ln\left(1-\frac{C}{C_0}\right)=\frac{d\alpha}{\theta_{im}v_m}+\ln\left(\frac{\theta_{im}}{\theta}\right)-\frac{\alpha}{\theta_{im}}t \qquad (16.79)$$

The θ_{im} and α can again be measured by plotting the ln(l − C/C_0) versus t. It should clearly understood that the assumption C_m=C_0 associated with Eqs. (16.76) to (16.79) may not be correct for a>0.

By Making Approximations

The partition coefficient "β" can be obtained by using the inverse modeling technique from a measured breakthrough curve. The β, f and ϕ_m are related by the following equation, which shows that from a known value of β the f and ϕ_m cannot be calculated directly:

$$\phi_m = [R\beta - f(R-1)] \tag{16.80}$$

If R is close to 1 then

$$\phi_m = \beta \tag{16.81}$$

For $R \neq 1$, the mobile water fraction (ϕ_m), which is the ratio of θ_m and θ, can be calculated from known field capacity water content and Eq. (16.74). A better option for obtaining the values of ϕ_m or β is to make some assumptions on f, which is defined as the fraction of sorption sites in mobile region. When soil is saturated and distribution of sorption sites is independent of the location in soil-water regions (Seyfried and Rao, 1987)

$$f = \phi_m = \beta \tag{16.82}$$

However, the assumption that more sites for adsorption are available in the immobile region is more appropriate (Nkedi-Kizza et al., 1982). This assumption is appropriate because the pores in immobile regions are smaller and have higher exposed surface area than in mobile region. Therefore, f can be assumed to vary from 0 to $\phi_m/2$ (Seyfried and Rao, 1987).

Aggregate Geometry Models

The nondimensional mass transfer parameter (ω) is not directly related to any specific soil characteristic or property and is difficult to determine. The a is a function of time of diffusion, sphere radius (particles constituting the porous medium), molecular diffusion coefficient, intraaggregate water content (θ_{im}), macroporosity (fraction of total porosity); therefore, apart from Eqs. (16.78) and (16.79), the α can be calculated for the known or assumed geometry of aggregates. For spherical aggregates α can be calculated as follows (Rao et al., 1980).

$$\alpha = \frac{D_e(1-f)\theta}{r^{20}}\alpha^* \tag{16.83}$$

where D_e is the effective diffusion coefficient, r is the radius of sphere, and α^* is time dependent variable. The α values of cubic aggregates can be obtained by replacing "a" with an equivalent spherical radius "r=0.6203l", where f is the length of the side of the cube (Rao et al., 1982). Another widely used formula for the estimation of α based on soil geometry is (van Genuchten, 1985; van Genuchten and Dalton, 1986):

$$\alpha = \frac{nD_e(1-f)\theta}{a_e^2} \tag{16.84}$$

where n is a geometry factor, and a_e is an average effective diffusion length. If a soil matrix, with overall conductivity of K_e, can be divided into a two-flow domain physical nonequilibrium model. The water contents of these flow regions are θ_A and θ_B for velocities υ_A and υ_B, respectively. For steady flow condition the a can be estimated as follows (Skopp et al., 1981):

$$\alpha = \frac{2K_e\theta_A(v_A - v_B)^2}{gdr_p\pi} \tag{16.85}$$

where d is the aggregate size (cm), r_p is the interaggregate pore size (cm), and g is acceleration due to gravity (cmh^{-2}). It should be remembered here that α values estimated using aggregate geometry models does not necessarily fit the measured breakthrough curves very well. The α values depend on the experimental conditions (Ma and Selim, 1998). In general α values increase with flow velocity probably as a result of turbulent mixing at high velocities (van Genuchten and Wierenga, 1977). However, α values decrease if greater pore connectivity exists in the flow domain (Skopp and Gardner, 1992).

16.20 Land Use Effects on Flow and Transport

The flow and transport properties of soils often vary with time due to the influence of land use and soil management practices. The soil remains mostly undisturbed under no-till, which enhances the organic matter accumulation at the soil surface and development of macropores (cracks between aggregates and pores). The macropore channels in no-till system increase the leaching of nutrients and pesticides by bypassing the water-filled micropores unless the sources are located within the soil micropores. These cracks increase the hydraulic conductivity of soil and decrease reactivity of dissolved chemicals due to the low pore surface area and short residence time. The increase in organic matter increases the reactivity of chemicals in the soil matrix and the soils start behaving as a multireaction, multiregion soil. It is important to know this shift in flow and transport processes due to macropores as failure to take these into account can lead to erroneous conclusions. For an example: In a macroporous soil system, a zero-tension lysimeter was installed at a 90-cm depth, which captured 50% of the applied pesticide leached out of root zone system via macropore channels. The analysis of soil samples at different depth increments showed very little traces of pesticides. Therefore, without having the knowledge of preferential flow of pesticides, an inaccurate conclusion that pesticides had limited mobility due to high degradation rates can be drawn. Similarly, an increase in organic matter provides kinetic adsorption sites for some solutes, which would lead to inaccurate results if lumped into instantaneous equilibrium adsorption terms (Wilson et al., 2000).

Example 16.1

Concentration of a solute is 30 mg/g of soil and bulk density is 1.35 Mg/m^3. Assuming steady flow conditions, solute free soil profile, and solute diffusion coefficient $3\times10^{-10}m^2/s$, calculate flux density at a vertical distance of 0.1 m and amount of solute in 1 ha that diffuses across this boundary in 2 months. (Hint: Use Fick's first law.)

Solution

Solute concentration=ρ_b * C_a=30 * 1.35=40.5 M/gm^3 or 4.05×10^7 mg/m^3
Concentration gradient at 0.1 m below soil surface

$\delta C/\delta z=\Delta C/\Delta z=(0–4.05\times10^7)/(0–0.1)=4.05\times10^8$ mg/m^4

The flux density of solute is obtained by using equation 7

$J=-(3\times10^{-10})*(4.05\times10^8)=-0.122$ mg $m^{-2}s^{-1}$

The negative sign implies that solute is moving downward. The total quantity of solute moved below 0.1 m in one month *(Q)* can be calculated as

$Q=0.122*10000*30*24*3600=3.16\times10^9 mgha^{-1}$

Example 16.2

Nitrate-N was applied in a field at volumetric moisture content of 0.35. If soil water flux density was $0.05cmd^{-1}$ and soil solution concentration of NO_3-N was $4mgL^{-1}$, calculate the pore water velocity and amount of NO_3-N leached per unit area by convective flow below the root zone in 2 days.

Solution

Pore water velocity=$v=q/\theta$=0.05/0.35=0.143 cm/d
The flux density for convective transport *(J_m)* can be calculated from equation 6.

$J_m=qC=0.05*4*1000/1000=2.0$ mg/m^2d

Therefore, amount of NO_3-N (Q) leached through root zone in 2 days

$Q=J_m*A*t=2*1*2=4$ mg

Example 16.3

Assuming steady condition and piston flow through a soil column at moisture content of $0.35cm^3cm^{-3}$, calculate the total time required to transport chloride from the bottom of the root zone to groundwater at 50 m below when average daily drainage rate is 0.25 m/d.

Solution

Total depth of water in the vadose zone=0.35*50=17.5 m The breakthrough time (total time required) to transport all the chloride to groundwater=17.5/0.25=70 d Alternately, pore water velocity of chloride *(v=q/θ)*=0.25/0.35=0.71 m/d Breakthrough time *(t*=L/v)*=50/0.71=70 d

Example 16.4

Using the information in Example 3, calculate the velocity and breakthrough time for chloride if bulk density of soil was 1.4 Mg/m^3 and the slope of equilibrium isotherm was 0.06 $m^3\ Mg^{-1}$.

Solution

The retardation factor *(R)*=1+*k*ρ_b/θ*=1 +0.06* 1.4/0.35=1.24 Average chloride velocity=0.25/(0.35* 1.24)=0.58 m/d The breakthrough time=50/0.58=86 days

PROBLEMS

1. In a repacked loam soil column with total porosity (ϕ of 0.5, the measured dispersivity *(λ)* was 1.2. Assuming that diffusion coefficient of solute in water (D_0) is 1 $cm^2\ day^{-1}$, calculate remaining parameters given in the table below.

Note: Tortuosity factor *(ξ)* is given as $\xi = \theta^{10/3}/\phi^2$ (known as the Millington– Quirk formula, 1961). Effective-dispersion diffusion coefficient *(D)* is given by $D_e=D_h+D_m$.

q ($cm.d^{-1}$)	θ	v ($cm.d^{-1}$)	ξ	D_h	D_m	D
0.2	0.25					
1	0.3					
2	0.35					
5	0.4					

2. Assume that average volumetric water content *(θ)* of soil is 0.2; and bulk density *(ρ_b)* is 1.5 g cm^{-1}. The average annual drainage rate *(dr)* is 0.5 myr^{-1}. If a pesticide, *Kd*=2cm^2g^{-1}, is applied to this soil, calculate how long (breakthrough time) it will take to move the pesticide to the groundwater at (L) 12 m depth.

3. Chloride solution was applied as a step input to a 10 cm long soil column initially saturated with water. The flux density of chloride *(q)* was 0.5 cm h^{-1}, and average water content of column was 0.45cm^3cm^{-3}. The chloride ETC can be plotted on an Excel spreadsheet with X-axis as pore volumes *(p)* and relative chloride concentration *(C/C_0)*. The pore volumes are 0.2, 0.4, 0.6, 0.8, 1.0, 1.2, 1.4, and 1.6 and corresponding C/C_0 are 0.01, 0.06, 0.15, 0.3, 0.54, 0.8, 0.96, and 0.99 respectively. Calculate the apparent diffusion coefficient *(D)* and retardation coefficient (R).

REFERENCES

Bear J. (1972). Dynamics of fluid in porous media. Elsevier Science, New York.
Bear J. and Y.Bachmat (1967). A generalized theory on hydrodynamic dispersion in porous media. Symp. Artificial Recharge Management Aquifers, Haifa, Int. Assoc. Sci. Hydrol., 72:7–36.
Biggar J.W. and D.R.Nielsen (1967). Miscible displacement and leaching phenomenon. Agronomy 11:254–274.
Bolt G.H. (1979) (ed.). Soil chemistry. B: Physio-chemical models. Elsevier Scientific Pub. Co., New York.
Bond W.J., B.N.Gardiner, and D.E.Smiles (1982). Constant flux adsorption of a tritiated calcium chloride solution by a clay soil with anion exclusion. Soil Sci. Soc. Am. J. 46:1133–1137.
Bresler E. (1973). Anion exclusion and coupling effects in a nonsteady transport through unsaturated soils: I. Theory. Soil Sci. Soc. Am. Proc. 37:663–669.
Butters G.L., W.A.Jury, and F.F. Ernst (1989). Field scale transport of bromide in an unsaturated soil. 1. Experimental methodology and results. Water Resour. Res. 25:1575–1581.
Cameron D.R. and A.Klute (1977). Convective–Dispersive solute transport with a combined equilibrium and kinetic adsorption model. WRR, 13(1): 183–188.
Clothier B.E., M.B.Kirkham, and J.E.Mclean (1992). In situ measurements of the effective transport volumes for solute moving through soil. Soil Sci. Soc. Am. J. 56:733–736.
Coats K.H. and B.D.Smith (1964). Dead end pore volume and dispersion in porous media. SPE J. 4:73–84.
De Josselin De Jong G. (1958). Longitudinal and transverse diffusion in granular deposits. Trans. Amer. Geophys. Union 59:67.
Ellsworth T.R., P.J.Shouse, T.H.Skaggs, J.A.Jobes, and J.Fargerlund (1996). Solute transport in unsaturated soil: experimental design, parameter estimation, and model discrimination. Soil Sci. Soc. Am. J. 60:397–407.
Fleming J.B. and G.L. Butters (1995). Bromide transport detection in tilled and nontilled soil:solute samplers vs. soil cores. Soil Sci. Soc. Am. J. 59: 1207–1216.
Flury M., W.A.Jury, and E.J.Kladivko (1998). Field scale solute transport in vadose zone: Experimental observations and interpretation. In: H.M. Selim and L. Ma (eds.), Physical Nonequilibrium in Soils. Ann Arbor Press, Michigan, p 349–365.
Fried J.J. and M.A.Combarnous (1971). Dispersion in porous media. Ad. Hydroci. 7:169–282.
Greenkorn R.A. (1983). Flow phenomena in porous media. Marcel Dekker Inc., New York and Basel, p 190.
Hamlen C.J. and R.G.Kachanowski (1992). Field solute transport across a soil horizon boundary. Soil Sci. Soc. Am. J. 56:1716–1720.
James R.V. and J.Rubin (1986). Transport of chloride ion in a water unsaturated soil exhibiting anion exclusion. Soil Sci. Soc. Am. J. 50:1142–1149.
Jaynes D.B. (1991). Field study of bromacil transport under continuous flood irrigation. Soil Sci. Soc. Am. J. 55:658–664.
Jaynes D.B., S.D.Logsdon, and R.Horton (1995). Field method for measuring mobile/immobile water content and solute transfer rate coefficient. Soil Sci. Soc. Am. J. 59:352–356.
Jury A.W. and K.Roth (1990). Transfer functions and solute movement through soil. Birkhaeuser Verlag, Basel, Germany.
Jury A.W., W.R.Gardner, and W.H.Gardner (1991). Soil physics, 5th Edition, John Wiley, New York. Torelli L. and A.E. Scheidegger (1972). Threedimensional branching type models of flow through porous media. J. Hydro. 15:23.
Kirkham D. and W.L.Powers (1972). Advanced soil physics. Wiley Interscience, John Wiley & Sons, Inc., New York.
Krupp H.K. and D.E.Elrick (1968). Miscible displacement in an unsaturated glass bead medium. Water Resour. Res. 4:809–815.

Krupp H.K., J.W.Biggar, and D.R.Nielsen (1972). Relative flow rates of salt and water in soil. Soil Sci. Soc. Am. Proc. 36:412–417.
Kutilek M. and D.R.Nielsen (1994). Soil Hydrology. Catena Verlag, CremlingenDestedt, Germany.
Lapidus L. and N.R.Amundson (1952). Mathematics of adsorption in beds. J. Phys. Chem. 56:584.
Ma L. and H.M.Selim (1998). Physical nonequilibrium in soils: modeling and application. In: H.M.Selim and L.Ma (eds.), Physical Nonequilibrium in Soils. Ann Arbor Press, Michigan, p 83–115.
Morisawa S., M.Horiuchi, T.Yamaoka, and Inoue Y. (1986). Evaluation of solute transport in unsaturated soil column by multicompartment flow model. (In Japanese) Proc. Environ. Sanitary Engg. Res. 22:9–22.
Nielsen D.R., M.Th.van Genuchten, and J.W.Biggar (1986). Water flow and solute transport processes in the unsaturated zone. Water Resour. Res., 22(9): 89S–108S.
Nkedi-Kizza P., J.W.Biggar, H.M.Selim, M.Th.van Genuchten, P.J.Wierenga, J.M.Davidson, and D.R.Nielsen (1984). On the equivalence of two conceptual models for describing ion exchange during transport through an aggregated oxisol. Water Resour. Res., 20(8): 1123–1130.
Nkedi-Kizza P., P.S.C.Rao, R.E.Jessup, and J.M.Davidson (1982). Ion exchange and diffusive mass transfer during miscible displacement through and aggregated Oxisol. Soil Sci. Soc. Am. J. 46:471–476.
Parker J.C. and M.Th.van Genuchten (1984a). Flux-averaged and volume-averaged concentrations in continuum approaches to solute transport. Water Resour. Res. 20(7):866–872.
Perkins T.K. and O.C.Johnston (1963). A review of diffusion and dispersion in porous media. Pet. Trans. AIME 228, SPEJ 70.
Pfannkuch H.O. (1962). Contribution a L'etude des deplacement de fluides miscible dans un milieu poreux. Rev. Inst. Fr. Petrol. 18(2):215.
Rao P.S.C., R.E.Jussup, D.E.Rolston, J.M.Davidson, and D.P.Kilcrease (1980). Experimental and mathematical description of nonadsorbed solute transfer by diffusion in spherical aggregates. Soil Sci. Soc. Am. J. 44(4):684–688.
Rao P.S.C., R.E.Jessup, and T.M.Addiscott (1982). Experimental and theoretical aspects of solute diffusion in spherical and nonspherical aggregates. Soil Sci. 133:342–349.
Roth K., W.A.Jury, H.Fluehler, and W.Attinger (1991). Transport of chloride through an unsaturated field soil. Water Resourc. Res. 27:2533–2541.
Selim H.M. (1992). Modeling the transport and retention of inorganics in soil. Adv. Agron. 47:331–384.
Selim H.M., J.H.Davidson, and R.S.Mansell (1976). Evaluation of a two-site adsorption desorption model for describing solute transport in soils. Proceedings Summer Computer Simulation Conference, Washington D.C., 444–448.
Seyfried M.S. and P.S.C.Rao (1987). Solute transport in undisturbed columns of an aggregated tropical soil: Preferential flow effects. Soil Sci. Soc. Am. J. 51: 1434–1444.
Shukla M.K. and G.Kammerer (1998). Comparison between two models describing solute transport in porous media with and without immobile water. Austrian Journal of Water Management 50(9/10):254–260.
Shukla M.K., F.J.Kastanek, and D.R.Nielsen (2000). Transport of chloride through water-saturated soil columns. The Bodenkulture, Austrian Journal of Agricultural Research 51(4):235–246.
Shukla M.K., F.J.Kastanek, and D.R.Nielsen (2002). Inspectional analysis of convective dispersion equation and application on measured BTCs. Soil Sci. Soc. of Am. J. 66(4): 1087–1094.
Shukla M.K., T.R.Ellsworth, R.J.Hudson, and D.R.Nielsen (2003). Effect of water flux on solute velocity and dispersion. Soil Sci. Soc. Am. J. 67:449–457.
Skopp J. and W.R.Gardner (1992). Miscible displacement: an interacting flow region model. Soil Sci. Soc. Am. J. 56:1680–1686.
Sposito G. (1989). The chemistry of soils. Oxford Press, p 277.
Taylor G.I. (1953). The dispersion of matter in solvent flowing slowly through a tube. Proc. R. Soc. London, Ser. A 219:189–203.

Toride N., F.K.Leij, and M.Th.van Genuchten (1993). A comprehensive set of analytical solutions for nonequilibrium solute transport with first-order and zero-order production. Water Resour. Res. 29(7):2167–2182.

Valocchi, A.J. (1985). Validity of local equilibrium assumption for modeling sorbing solute transport through homogeneous soils. Water Resour. Res. 21: 808–820.

Van de Pol R.M., P.J.Wierenga, and D.R.Nielsen (1977). Solute movement in field soil. Soil Sci. Soc. Am. J. 41:10–13.

van Genuchten M.Th. (1985). A general approach for modeling solute transport in structured soils. Proc. 17 The Int. Congress. IAH, Hydrogeology of Rocks of Low Permeability. Jan 7–12, 1985, Tucson, AZ. Mem. Int. Assoc. Hydrogeol. 17:512–526.

van Genuchten M.Th. and F.N.Dalton (1986). Models for simulating salt movement in aggregated field soils. Geoderma. 38:165–183.

van Genuchten M.Th. and P.J.Wierenga (1976). Mass transfer studies in sorbing porous media I Analytical solutions. SSSA Proceedings 40(4):473–480.

van Genuchten M.Th. (1981). Non-equilibrium transport parameters from miscible displacement experiments. Research report 119, USD A, US Soil salinity lab Riverside, California,

van Genuchten M.Th. and J.C.Parker (1984). Boundary conditions for displacement experiments through short laboratory soil columns. Soil Sci. Soc. Am. J. 48: 703–708.

van Genuchten M.Th. and P.J.Wierenga (1977). Mass transfer studies in sorbing porous media. II. Experimental evaluation with tritium (^3H_2O). Soil Sci. Soc. Am. J. 41:272–277.

van Genuchten M.Th. and P.J.Wierenga (1986). Solute dispersion coefficients and retardation factors. In: A. Klute, (ed.), Methods of Soil Analysis, Part 1: Physical and Mineralogical Methods, 2nd Edition, American Society of Agronomy, Madison, Wisconsin.

van Genuchten M.Th. and W.J.Alves (1982). Analytical solutions of the onedimensional connective dispersion solute transport equation. USDA Tech. Bull. 1661.

Van Wesenbeck I.J. and R.G.Kachanowski (1991). Spatial scale dependence of in situ solute transport. Soil Sci. Soc. Am. J. 55:3–7.

White R.E., L.K.Heng, and R.B.Edis (1998). Transfer function approaches to modeling solute transport in soils. In: H.M. Selim and L. Ma (eds.), Physical nonequilibrium in soils. Ann Arbor Press, Michigan, p 311–346.

White R.E., J.S.Dyson, Z.Gerstl, and B.Yaron (1986). Leaching of herbicides through undisturbed cores of a structured clay soil. Soil Sci. Soc. Am. J. 50: 277–283.

Wilson J.L. and L.W.Gelhar (1974). Dispersive mixing in a partially saturated porous medium, Persons Laboratory Report 191, Massachusetts Institute of Technology, Cambridge.

Wilson G.V., H.M.Selim, and J.H.Dane (2000). Flow and transport processes. In: H.D. Scott, (ed.), Water and Chemical Transport in Soils of the Southeastern USA. SCSB-395. Department of Plant and Soil Sciences, Oklahama State University.

17
Soil Temperature and Heat Flow in Soil

17.1 TEMPERATURE

Temperature is a measure of the thermal state of a body with respect to its ability to transfer heat. It is also defined as the measure of intensity or potential energy or heat. Temperature is the driving force for heat flow as pressure head is for water flow. Temperature is measured in three scales: Celsius (°C), Fahrenheit (°F), and Kelvin (K). The conversion from one scale to another is given in Table 17.1.

17.2 THE DEVELOPMENT OF THERMOMETER AND TEMPERATURE SCALES

One of the first attempts to make a standard temperature scale occurred about 170 AD, when Galen proposed a standard neutral temperature made up of equal quantities of boiling water and ice with four degrees of heat and cold on either side of this temperature, respectively. The earliest device used to measure the temperature was known as a "thermoscope" and consisted of a glass bulb having a long tube, which extended downward into a container of colored water. Before filling the liquid, some of the air in the bulb was

TABLE 17.1 Mathematical Expressions and Relations for Temperature Scales

Temperature scales	Mathematical formula
Celsius (°C)	°C=(5/9)*(°F−32)
Fahrenheit (°F)	°F=(9/5)*°C+32
Kelvin (K)	K=°C+273.15

removed, causing the liquid to rise into the tube. As the remaining air in the bulb was heated or cooled, the level of the liquid in the tube would vary reflecting the change in

the air temperature. An engraved scale on the tube allowed for a quantitative measure of the temperature fluctuations.

The first sealed thermometer using liquid rather than air as the thermometric medium was developed for Ferdinand II in 1641. The thermometer was a sealed alcohol-in-glass device, with 50 “degree” marks on its stem, but no “fixed point” was used to zero the scale. This device was referred to as a “spirit” thermometer. Robert Hook (1664) used a red dye in the alcohol and the scale needed only one fixed point, for which every degree represented an equal increment of volume equivalent to about 1/500 part of the volume of the thermometer liquid, which was the freezing point of water. Hook demonstrated that a standard scale could be established for thermometers of a variety of sizes. Hook’s original thermometer was known as the standard of Gresham College, and was used by the Royal Society until 1709.

Ole Roemer of Copenhagen, Denmark, developed the thermometer scale in 1702 based upon two fixed points: snow (or crushed ice) and the boiling point of water, and recorded the daily temperatures at Copenhagen in 1708 and 1709. Gabriel Fahrenheit, an instrument maker in Amsterdam, The Netherlands, was the first to use mercury as the thermometric liquid in 1724. Mercury’s thermal expansion is large and uniform, and does not stick to the glass, and remains a liquid over a wide range of temperatures. The silvery appearance also makes it easy to read. Fahrenheit measured the boiling and freezing points of water to be 212 and 32, respectively, and designated temperatures in degrees Fahrenheit (°F).

In 1745, Carolus Linnaeus of Uppsala, Sweden, described the freezing point of water as zero, and the boiling point as 100, making it a “centigrade” (one hundred steps) scale. Anders Celsius (1701–1744) used the reverse scale in which 100 represented the freezing point and zero the boiling point of water, still, with 100 degrees between the two defining points. In 1948 use of the centigrade scale was dropped in favor of a new scale using degrees Celsius (°C). A degree Celsius equals the same temperature change as a degree on the ideal-gas scale. An “ideal gas” is one whose physical behavior is accurately described by the ideal-gas equation*. On the Celsius scale, the boiling point of water at standard atmospheric pressure is 99.975°C in contrast to the 100 degrees defined by the centigrade scale.

In 1780, J.A.C.Charles, a French physician, showed that for the same increase in temperature, all gases exhibited the same increase in volume. Because the expansion coefficient of gases is about the same, it is possible to establish a temperature scale based on a single fixed point rather than the two fixed-point scales, such as the Fahrenheit and Celsius scales. This brings us back to a thermometer that uses a gas as the thermometric medium.

P.Chappuis in 1887 conducted extensive studies of gas thermometers with constant pressure or with constant volume using hydrogen (H_2), nitrogen (N_2), and carbon dioxide (CO_2) as the thermometric medium. Based on his results, the Comité International des Poids et Mesures adopted the constant-volume hydrogen scale based on fixed points at the ice point (0°C) and the steam point (100°C) as the practical scale for international meteorology.

17.3 MEASUREMENT OF TEMPERATURE

The temperature of a substance (such as soil) is generally measured indirectly by measuring a property that responds to changes in its heat content. Some of these instruments are the liquid-in-glass thermometer, electric resistance thermometer, bimetallic thermometer, thermocouple, and remote-sensing thermometer (www.temperatures.com; Childs et al., 2000; Scott, 2000).

17.3.1 Liquid-in-Glass Thermometer

The liquid-in-glass thermometer is placed in close contact with soil or any substance, the conduction of heat between thermometer and its surrounding soil causes the change in volume of liquid in the glass thermometer (Childs et al., 2000; Scott, 2000). The traditional liquid-in-glass thermometer consists of a reservoir and capillary tubes and is based on the design proposed by Danial Fahrenheit in 1714. This type of thermometer is used very commonly in the field and is sufficient for a reliable measurement of soil temperature provided good contact between reservoir and soil is

* PV=nRT, where P is the pressure (atm), V is the volume (m^3), n is number of moles, T is temperature (K), and R universal gas constant.

ensured. The accuracy of these devices ranges from ±0.01 to ±4°C. For the measurement of maximum and minimum temperatures, alcohol, toluene, or mercury is used as thermometric liquid. Since mercury vapors are toxic to human (ATSDR, 1999), cheaper resistance devices giving a digital readout have replaced mercury-in-glass thermometers.

17.3.2 Electric Resistance Thermometer

Electric methods are mostly based on the thermoelectric effect of temperature or change in resistance of a metal with a change in temperature. The motion of free electrons and atomic lattice vibrations are temperature dependent, which makes it possible to relate the resistance of a conductor to temperature. Resistance thermometers consist of a thin platinum or nickel wire, which is spiraled on a cylinder. The resistance measured using a bridge circuit generally increases by 0.4–0.5% per °C rise in temperature. A semiconductor known as a thermistor is a special type of resistance thermometer whose resistance decreases exponentially with an increase in temperature as follows (Scott, 2000):

$$R = B\exp\left(\frac{a}{T}\right) \tag{17.1}$$

where a and B are constants and T is the absolute temperature. The advantage of electric thermometers is that they can be easily used for continuous and rapid temperature measurements and can be highly accurate (Childs et al., 2000). However, these thermometers need to be frequently calibrated during use (Scott, 2000).

17.3.3 Bimetallic Thermometer

Bimetallic thermometers have two metals strips, which are joined together. These strips have different thermal expansion coefficients. The strips are also connected to a pointer. When temperature changes, the metal strips get deformed, which moves the pointer on a temperature scale. These thermometers are commonly used in thermographs and their accuracy is few tenths of a °C. An advantage of these devices is that they do not require a power supply (Childs et al., 2000; Scott, 2000).

17.3.4 Thermoelectric Thermometer

Sir William Siemens, in 1871, proposed a thermometer whose thermometric medium is a metallic conductor, whose resistance changes with temperature. The element platinum does not oxidize at high temperatures and has a relatively uniform change in resistance with temperature over a large range. The platinum resistance thermometer is now widely used as a thermoelectric thermometer and covers the temperature range from about −260°C to 1235°C. It defines the international temperature scale between the triple point of hydrogen (H_2), 13.8023 K, and freezing point of silver, 1234.93 K, within an accuracy of ±0.002 K. Errors associated with platinum resistance thermometers are self heating, oxidation, corrosion, and strain of sensing element (Childs et al., 2000). If accuracy is less critical, a cheaper form of resistance thermometer known as a "thermistor" can be used. This utilizes a semiconductor (e.g., mixtures of oxides of nickel, magnesium, iron, copper, cobalt, manganese, titanium, etc.) in place of platinum. The accuracy of these devices for commercial application is ±1°C.

17.3.5 Thermocouple

Thermocouple, the most widely used soil temperature measurement instrument, is made up of two wires of different metals (commonly copper-constantan, iron-constantan, or chromel-constantan) welded together at two places with the welds kept at different temperatures. The temperature difference causes a roughly proportional electric potential difference between the welds and current flows through the circuit formed by two wires. This effect is known as the thermoelectric effect. For measurement of soil temperature, one of the welds is kept at reference temperature while the other is kept in contact with soil. The compensation method measures the thermoelectric potential difference, and a galvanometer, the thermoelectric current between welds. Thermocouples are less economic, robust, and capable of monitoring temperatures between −270 and 3000°C. The sensitivity and speed of these devices is sufficient for many applications but are less accurate than resistance temperature devices (Childs et al., 2000; Scott, 2000).

17.3.6 Remote Sensing Thermometer

Temperature measurement devices based on thermal radiation monitoring can measure temperatures from 50 to 6000 K (Childs et al., 2000). Infrared thermometry is the most popular methods of estimating the temperature of the surfaces of soil, plant leaves, and crop canopies. According to the Stefan–Boltzmann equation the infrared radiations emitted by the surface are expressed as follows [see also Eqs. (17.15) and (17.16)]

$$Rl=e\sigma T^4 \tag{17.2}$$

where R_l is the long wave radiation, e is emissivity, which is close to 1 for most soil and plant surfaces, σ is Stefan–Boltzmann constant ($5.675\times10^{-8}\mathrm{Wm^{-2}K^{-4}}$), and T is absolute temperature (Scott, 2000). An infrared measurement system comprises a source, a medium through which heat energy is transferred (e.g., gas), and a measurement device (e.g., optical system, a detector, a control and analysis system).

17.4 TEMPERATURE AS A THERMODYNAMIC PROPERTY (see also Chapter 14)

Experiments with gas thermometers have shown that there is very little difference in the temperature scale for different gases. Thus, it is possible to set up a temperature scale that is independent of the thermometric medium if it is a gas at low pressure. In this case, all gases behave like an "ideal gas" and have a very simple relation between their pressure, volume, and temperature:

$$PV=(\text{constant})T \tag{17.3}$$

where P is partial pressure of gas, V is volume of gas, T is temperature (also known as thermodynamic temperature), which is defined as the fundamental temperature and whose unit is the Kelvin (K), named after Lord Kelvin. Note that there is a naturally defined zero on this scale that is the point at which the pressure of an ideal gas is zero, making the temperature zero. With this as one point on the scale, only one other fixed point needs to be defined. In 1933, the International Committee of Weights and Measures adopted this fixed point as the triple point of water, the temperature at which water, ice, and water vapor coexist in equilibrium; its value is set as 273.16 K.

17.4.1 Entropy

Entropy *(S_e)* is a thermodynamic quantity, which is a measure of the degree of disorder within any system. The greater the degree of disorder, the higher the S_e. For an increase in disorder, S_e is positive and has the units of joules per degree K per mole. The entropy has a standard that is fixed by the third law of thermodynamics (see the following section).

17.4.2 Enthalpy

Enthalpy *(H)* is a thermodynamic state function, generally measured in kilojoules per mole. In chemical reactions the enthalpy change (ΔH) is related to changes in the free energy (ΔG) and entropy *(ΔS_e)* by the Gibbs equation:

$$\Delta G=\Delta H-T\Delta S_e \tag{17.4}$$

The enthalpy of an element has an internationally defined value at 298.15 K and 101.32 kPa and its entropy is zero at 0K and 101.32 kPa. The temperature that is most often used for recording thermodynamic data is 298.15 K, and by international convention the enthalpy of a pure element at 298.15 K and standard pressure is zero.

17.5 HEAT AND THERMODYNAMICS

Heat is the kinetic energy of random thermal motion of soil particles. Prior to the nineteenth century, it was believed that the sense of how hot or cold an object felt was determined by how much "heat" it contained. Heat was envisioned as a liquid that flowed from a hotter to a colder object, this weightless fluid was called caloric, and no distinction was made between heat and temperature. Black was the first to distinguish between the quantity (caloric) and the intensity (temperature) of heat. Joule (1847) conclusively showed that heat was a form of energy.

The zeroth law of thermodynamics states that if two bodies (e.g., masses of soil; *A* and *B*) are at the same temperature, and a third body *C* has the same temperature as body *B*, then the temperature of body *C* is equal to the temperature of body *A*.

Temperature $A=B=C$

(17.5)

The first law of thermodynamics is the conservation of energy and it states, "When heat is transformed into any other form of energy, or when other forms of energy are transformed into heat, the total amount of energy (heat plus other forms) in the system (plus surrounding) remains constant." To express it another way, the law states, "It is in no way possible either by mechanical, thermal, chemical, or other means, to obtain a perpetual motion machine; i.e., one that creates its own energy." At the same time, it is not possible to construct a cyclic machine that does nothing but withdraw heat energy and converts it into mechanical energy. No cyclic machine can convert heat energy wholly into other forms of energy, because efficiency of a cyclic machine can never be 100%. In the simplest form, the first law states "energy can neither be created nor destroyed." It can change from one form to another, for example, electricity to heat, heat that can boil water and make steam, hot steam that can push a piston (mechanical energy) or turn a turbine that makes electricity, which can be changed into light (in a light bulb) or can change to sound in an audio speaker system, and so forth. If the total energy of a system is *E*, then between any two equilibrium states *(E_1* for system 1 and E_2 for 2), the change in internal energy is equal to the difference of heat transfer *(Q)* into a system and work done *(W)* by the system

$$E_2-E_1=Q-W \tag{17.6}$$

A process, which does not involve heat transfer, is known as an adiabatic process. The second law of thermodynamics implies that there is an irreversibility of certain processes—that of converting all heat into mechanical energy. The law states that "there exists useful state variable called entropy *(S_e)* and the change in entropy is equal to the

heat transfer divided by the temperature." For a given physical process, the entropy of the system and the environment will remain constant if the process can be reversed.

$$\Delta S_e = \frac{\Delta Q}{T} \tag{17.7}$$

If we denote the initial and final states of the system by "*i*" and "*f*", then for a reversible system the change in entropy is zero (i.e., $S_{ef}=S_{ei}$) and for a reversible system the entropy will increase (i.e., $S_{ef}> S_{ei}$).

An example of a reversible process is ideally (no boundary layer losses) forcing a flow through a constricted pipe. As the flow moves through the constriction, the pressure, temperature and velocity would change, but these variables would return to their original values downstream of the constriction. The state of the gas would return to its original conditions and the change of entropy of the system would be zero. The second law states that if the physical process is irreversible, the entropy of the system and the environment must increase and the final entropy must be greater than the initial entropy. An example of an irreversible process is when a warm soil is kept in contact with a cold one and after some time both achieve the same equilibrium temperature. If we then separate two soils, they do not naturally return to their original (different) temperatures. The process of bringing them to the same temperature is irreversible.

The third law of thermodynamics was formulated by Walter Nernst and is also known as the Nernst heat theorem. The law states, "at absolute zero, all bodies have the same entropy." In other words, a body at absolute zero could exist in only one possible state, which possesses a definite energy, called the zero-point energy. This state is defined as having zero entropy, which is the entropy of a pure perfect crystal at 0K. At 0K, the atoms in a pure perfect crystal are aligned perfectly and do not move. Moreover, there is no entropy of mixing since the crystal is pure. For a mixed crystal containing the atomic or molecular species *A* and *B*, there are many possible arrangements of *A* and *B* and there is, therefore, entropy associated with the arrangement of the atoms/molecules.

17.5.1 Heat Capacity

The amount of temperature change in a body in response to heat adsorption or release is known as heat capacity. There are two types of heat capacities. The gravimetric heat capacity (C_g) is "the amount of heat energy required to raise the temperature of 1 kg of a substance by 1 K." The volumetric heat capacity (C_v) is "the amount of heat required to raise the temperature of 1 m3 of a substance by 1 K." The units of C_g and C_v in SI system are $Jkg^{-1}K^{-1}$ and $Jm^{-3}K^{-1}$, respectively. These two heat capacities are related by soil bulk density (ρ_b) as follows

$$Cg*\rho b=C_v \tag{17.8}$$

The specific heat of a substance is the ratio of the heat capacity of substance and water, and is dimensionless (see also the section on heat capacity of soils).

17.5.2 Blackbody

A blackbody is assumed to satisfy the ideal conditions, such as, (i) absorbs all incident radiation regardless of wavelength and direction, (ii) for a prescribed temperature and wavelength, no surface can emit more energy than a blackbody, and (iii) radiation emitted by a blackbody is a function of wavelength and is independent of direction. A blackbody is also known as a diffuse emitter.

17.6 FACTORS AFFECTING INSOLATION AT THE SOIL SURFACE

Radiations received at the soil surface are affected by a number of physical factors, which include vegetation, albedo, exposure, distribution of land and water, etc.

17.6.1 Vegetation

Vegetation cover buffers the soil beneath against sudden fluctuations in temperature. Bare soil is unprotected from the direct rays of the Sun and gets warm during the day and loses heat to atmosphere during the night. However, a good vegetative cover intercepts significant amount of solar radiation and prevents soil from getting warmer in summer. During winter or cold seasons, it prevents soil from losing heat as well, thereby reducing the daily variation of soil temperature as well as frost penetration and depth of freezing. The vegetation alters the soil energy balance in a number of ways, which include (i) altering albedo, (ii) insulating soil surface to prevent heat exchange, (iii) reducing depth of penetration of solar radiation, and (iv) increasing the removal of latent heat by evapotranspiration. Application of mulches on soil surface also alters the heat exchange in bare soil. The light colored mulches transmit short wave thermal energy to soil but prevent the loss of long wave thermal radiation and keep the soil warm by producing a green house effect.

17.6.2 Albedo

The fraction of all incoming solar radiations reflected back into space at the crop or soil surface is known as albedo. Albedo depends upon the nature of soil surface, angle of sunlight, and latitude. The albedo increases significantly with the distance from the equator. Water surfaces generally reflect 10% of the incoming radiations and therefore have lower albedo as compared to crop or soil surface. The albedo for canopy surfaces ranges from 5% for forest canopies to 25% for nonequatorial crops at full ground cover (Jury et al., 1991). The color of the soil is an important factor and affects the amount of reflection, for example, a light-colored soil has higher albedo than a dark-colored soil. Similarly a dry soil has higher albedo than a wet soil. The value of albedo for some soils and crops is presented in Table 17.2.

17.6.3 Latitude

The angle at which the Sun's rays meet the earth influences the amount of radiation received per unit area because of two reasons: (i) the albedo is high because of the angle, and (ii) radiation is subject to higher scattering reflection and adsorption, since they move through more atmospheres. Albedo is the highest in polar areas, decreases slightly in the middle latitudes, and is the lowest in tropical regions.

17.7 SOIL TEMPERATURE

Soil temperature is one of the most important factors affecting plant growth. Until soil reaches a certain critical temperature neither seeds

TABLE 17.2 Albedo from Soil, Forest, and Crops

Cover/surface	Albedo (%)	Reference
Light sand (Dry)	30–60	Geiger (1965)
Serozem (Dry)	25–30	Chudnovskii (1966)
Serozem (Wet)	10–12	Chudnovskii (1966)
Chernozem (Dry)	14	Chudnovskii (1966)
Chernozem (Wet)	8	Chudnovskii (1966)
Clay (Dry)	23	Chudnovskii (1966)
Clay (Wet)	16	Chudnovskii (1966)
Forest	5–20	Geiger (1965)
Corn (New York)	23.5	Chang (1968)
Sugar cane (Hawaii)	5–18	Chang (1968)
Pineapple (Hawaii)	5–8	Chang (1968)
Potato (Russia)	15–25	Chang (1968)

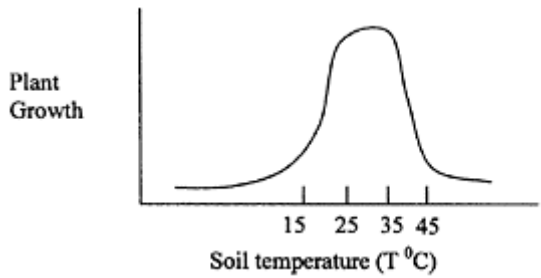

FIGURE 17.1 A graph of plant growth with soil temperature.

germinate nor plants have a normal growth because it affects root and shoot growth and availability of water and nutrients (Fig. 17.1). The optimum range of soil temperature for plant growth is between 20 and 30°C. The rate of plant growth declines drastically when temperature is less than 20°C (suboptimal) and above 35°C (supraoptimal) (Figs. 11.2–11 A). Further, all soil processes are temperature dependent. Consequently, the thermal regime of soil strongly influences the edaphic environment. The release of soil nutrients for root uptake is also dependent upon soil temperature regime. The biological processes (such as respiration by plants) are temperature dependent. Respiration rate (R_T) at a temperature (T) is expressed as follows:

$$R_T = R_0 Q_{10}^{(T-T_0)/10} \tag{17.9}$$

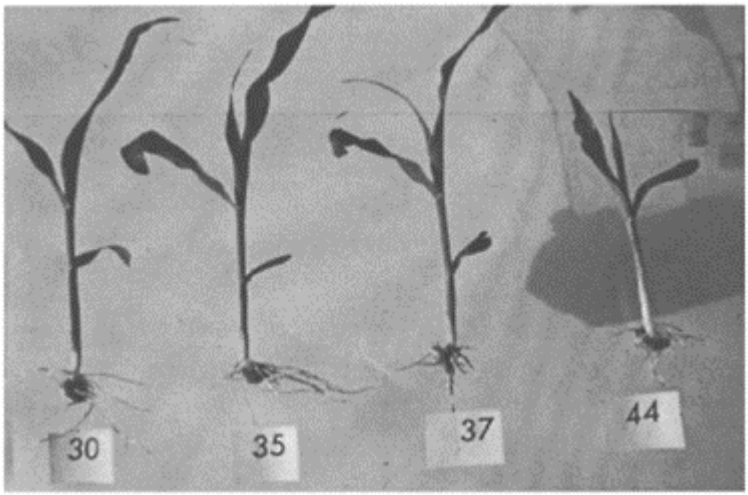

FIGURE 17.2 Corn seedling growth in relation to constant soil temperature maintained from 30 to 44° C in the root zone. (From Lal, 1972, greenhouse experiments.)

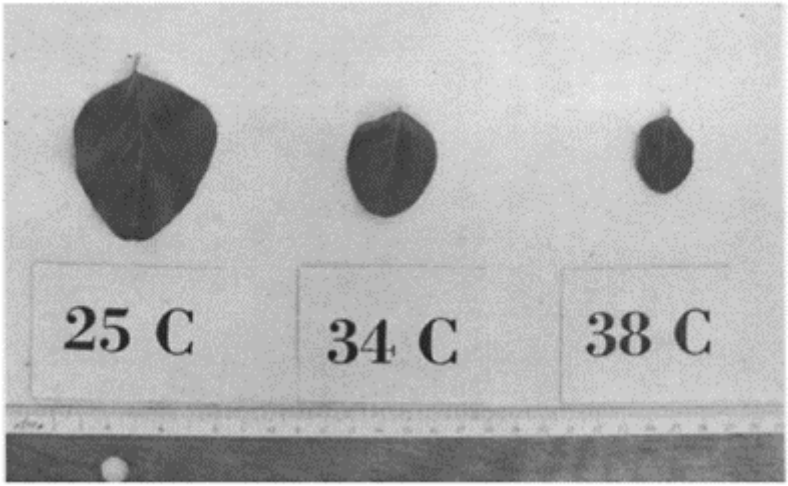

FIGURE 17.3 Soybean leaflets of seedlings grown at constant soil temperature of 25 to 38°C. (From Lal, 1972, greenhouse experiments.)

where R_0 is rate at reference temperature T_0, Q_{10} is the factor which relates respiration to each 10°C change in temperature. The reaction rate (K_{rea}) in soil is mostly described by the Arrhenius equation as follows:

$$K_{\text{rea}} = A \exp\left(-\frac{E}{RT}\right) \tag{17.10}$$

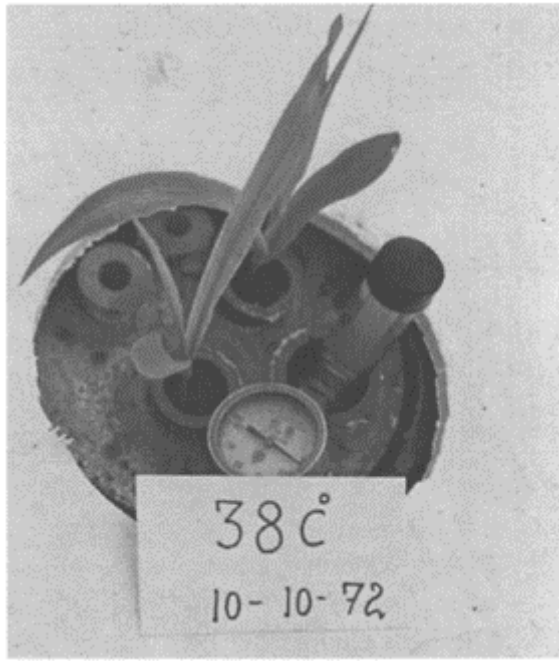

FIGURE 17.4 Chloratic symptoms of nutrient imbalance in corn seedlings grown at constant soil temperature of 38°C. (From Lal, 1972, greenhouse experiments.)

where A is the preexpopnetial factor, E is activation energy (J), R is gas constant (8.314 $Jmol^{-1}K^{-1}$), and T is absolute temperature. A plot of $\log K_{rea}$ vs. $1/T$ provides the values of empirical constants E (as the slope) and A (as the intercept).

Soil-water movement, soil-water availability, evaporation, and aeration are also governed by soil temperature. Heat stored near the soil surface has a strong influence on evaporation from soil. A drier soil warms up relatively more quickly and cools down faster than wetter soil because heat capacity of water is several times more than that of soil. Soil temperature also influences the properties of water, such as surface tension, and to a lesser degree, viscosity and density (Table 17.3). Hence, soil-water characteristic curves and hydraulic conductivity functions are also temperature dependent. Bouyoucus (1915) was among the first to observe water movement caused by the soil temperature gradient. He imposed temperature gradients across soil columns, which were at different water contents and contained different soil materials. He found that the difference in water between two halves of column was dependent on both soil material and initial temperature.

Soil temperature varies as a result of radiant, thermal, and latent heat energy exchange processes, which take place primarily through the soil

TABLE 17.3 Density and Viscosity of Water at Various Temperatures

Temperature (°C)	Density (g cm^{-3})	Viscosity (cp)
0	0.99987	1.787
3.98	1.00	1.568
5	0.9999	1.519
10	0.9997	1.307
20	0.9982	1.002
30	0.9957	0.7975
50	0.988	0.5468
80	0.971	0.3547
100	0.9584	0.2818

Source: Adapted from Handbook of Chemistry and Physics, 1988–89.

surface. Soil characteristics, which govern temperature regime, include bulk density, degree of wetness, soil heat capacity, and thermal sources and sinks present in soil matrix.

17.8 SOIL TEMPERATURE REGIMES

Soil temperature continuously varies in response to the changing meteorological regimes acting upon the soil atmosphere interface. The meteorological regimes are characterized by periodic succession of days and nights and winters and summers. Daytime heating is by short-wave radiation from the sun and sky, whereas nighttime cooling is from long-wave radiation emitted by soil. The temperature regimes of soil surface have two cyclical periods, namely diurnal and annual cycles.

17.8.1 The Diurnal Cycle

The variations in soil temperature owing to daytime heating and night-time cooling are known as diurnal variations. In the morning before sunrise, the minimum temperature of soil is the lowest at surface and increases with increase in depth. Similarly, the temperature continues to rise in the lower layers even after the top layer starts to cool down. However, the amplitude of the diurnal wave continues to decrease with soil depth (Fig. 17.5). The amplitude of the surface temperature fluctuation is the range from maximum or minimum to the average temperature (Fig. 17.5).

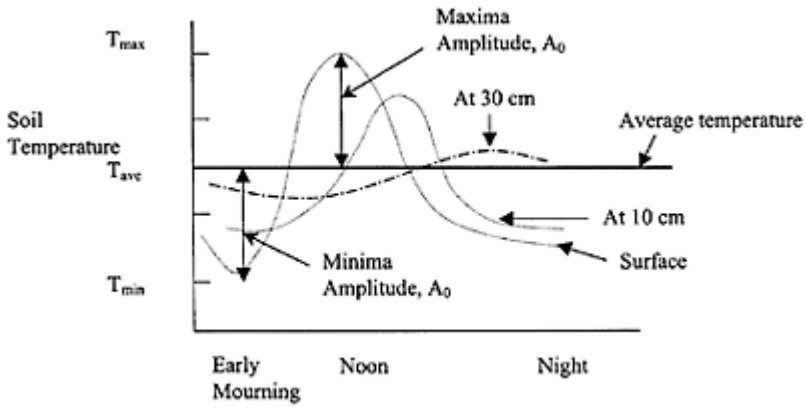

FIGURE 17.5 Schematic of diurnal variations in temperature measured at different depths.

17.8.2 The Annual Cycle

The annual variations in soil temperature result from the variations in short-wave radiation throughout the year. As one goes farther away from the equator, the annual variations in soil temperatures become significant. The summer months in June and July in the Northern Hemisphere represent the peak of global radiations and temperatures, whereas winter months have effects similar to nocturnal daily temperatures. During summer months, the soil temperature at surface is less than that of deeper layers (Fig. 17.6) (Smith, 1932).

The diurnal and seasonal variations of heat can be mathematically represented by assuming that soil temperature oscillates as a pure harmonic (sinusoidal) function of time around an average temperature. Let us also assume that average temperature of soil for all depths is the same. Assuming starting temperature as 0°C, the temperature at the soil surface and at any time *t* [T(0, *t*)] can be expressed as

$$T(0,t) = \overline{T} + A_0 \sin \omega t \tag{17.11}$$

where A_0 is the amplitude of surface temperature fluctuation, *to* is the angular or radial frequency (1 radian=57.3 degrees), which is 2π times the actual frequency, $\overline{T}$ is the average temparture and f is time. Assuming that at infinite depth *(z=∞),* the temperature is constant and equal to $\overline{T}$ (Fig. 17.5). Therefore, temperature at any depth *[T(z, t)]*

$$T(z,t) = \overline{T} + A_z \sin(\omega t + \phi(t)) \tag{17.12}$$

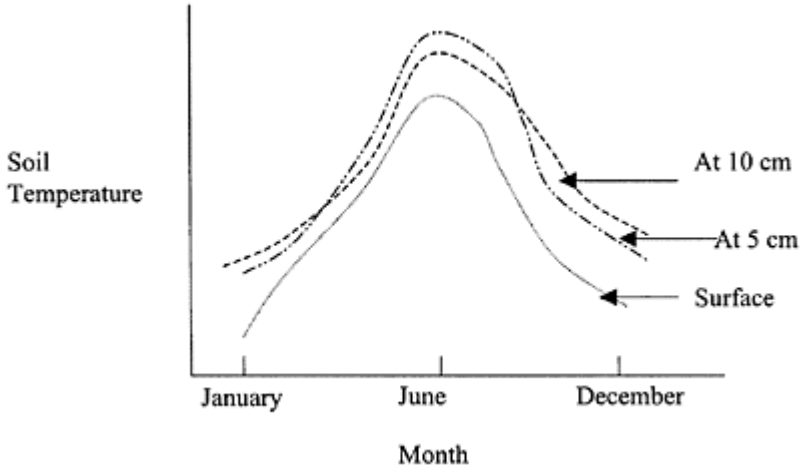

FIGURE 17.6 Schematic of annual variations in temperature measured at different depths in the Northern Hemisphere.

where A_z the amplitude at depth z and $\phi(z)$ are the functions of z, but not time. Incorporating the characteristic depth, also known as damping depth *(d)*, which is defined as the depth at which temperature amplitude decreases to the fraction $1/e^* A_0$, or $1/2.718^* A_0$, or $0.37^* A_0$, provides the following equation

$$T(z,t) = \overline{T} + \frac{A_0 \sin(\omega t + \phi(t))}{e^{z/d}} \tag{17.13}$$

The damping depth is also related to the thermal properties of the soil and the frequency of temperature fluctuation by the following relationship

$$d = \left(\frac{2k_t}{C_v \omega}\right)^{1/2} = \left(\frac{2D_T}{\omega}\right) \tag{17.14}$$

where C_v is volumetric heat capacity and D_T is thermal diffusivity of soil.

17.8.3 Soil Temperature Classes

Based upon the mean annual soil temperature, soil temperature regime is expressed in six categories (SSSA, 1987) namely pergelic, cryic, frigid, mesic, thermic, and hyperthermic (Table 17.4). In pergelic soils, mean annual temperature is lower, whereas in cryic soils, it is higher than 0°C. If mean annual temperature is lower than 8°C, the soils are known as frigid,

TABLE 17.4 Classes of Soil Temperature According to Taxonomy of Soils

Class	Mean annual temperature	Remarks
Pergelic	<0°C	Permafrost is present
Cryic	0°C< T<8°C	Mean $(T_{summer}-T_{winter})$=5°C at depth 0.5 m
Frigid	<8°C	Mean $(T_{summer}-T_{winter})$>5°C at depth 0.5 m
Mesic	8°C<T<15°C	Mean $(T_{summer}-T_{winter})$>5°C at depth 0.5 m
Thermic	15°C<T<22°C	Mean $(T_{summer}—T_{winter})$>5°C at depth 0.5 m
Hyperthermic	>22°C	Mean $(T_{summer}-T_{winter})$> 5°C at depth 0.5 m

Source: Modified from SSSA, 1987; Scott, 2000.

otherwise as mesic, provided mean annual temperature is below 15°C. For isofrigid, isomesic, isothermic, and isohyperthermic soils, the temperature differs by less than 5°C.

17.9 HEAT TRANSFER IN SOIL

There are three principle heat transport processes: radiation, conduction, and convection.

17.9.1 Radiation

Radiation is the process of heat transfer in which the emission of energy is expressed in the form of electromagnetic waves. The energy of the radiation field can also be transmitted through a vacuum since it does not require a carrier. The energy travels as discrete packets called quanta or photons, whose energy content depends on their wavelength or frequencies. According to the Stefan–Boltzmann law, the total energy emitted by a body, Ji, integrated over all wavelengths is proportional to the fourth power of the absolute temperature of the body, T, and can be expressed as below:

$$J_t=\sigma AT^4 \tag{17.15}$$

where A is the cross-sectional area of body (m^2), and a is the Stefan– Boltzmann constant and in SI units is expressed as 5.675×10^{-8} $Wm^{-2}K^4$. Eq. (17.15) gives the maximum energy flux that can leave a surface area A at any absolute temperature T. The ratio of radiant energy emitted by soil and maximum amount of radiant energy emitted $(\varepsilon_s/\varepsilon_b)$ is known as emissivity coefficient, which equals one for a perfect emitter. Normally a blackbody transmits the maximum and is known as a perfect emitter. Soils emit much less radiant energy. The ε varies as a function of the wavelength of radiation and serves as a correction factor or indicator of the efficiency of natural resources. Equation (17.15) can be modified to Eq. (17.16):

$$J_t=\varepsilon\sigma AT^4 \tag{17.16}$$

The T also determines the wavelength distribution of the emitted energy and is inversely proportional to maximum radiation intensity, λ_m, micrometers (μm), which is also known as Wien's law.

$$\lambda_m=2900/T \tag{17.17}$$

Assuming the temperature of the soil as 300 K, the radiations emitted by soil surface [Eq. (17.15)] have peak intensity at about 10 μm [refer to Eq. (17.17)] and its wavelength distribution is over the range of 3–50 μm, which falls in the infrared region. The Sun is a blackbody and has a temperature of 6000 K. The radiation emitted by the Sun has a peak intensity of about 500 nm [2900/6000]. The Sun's radiation includes a visible light range from 400 to 700 nm [400–425—Violet; 425–490—blue; 490–575—green; 575–585—yellow; 585–650—orange; 650–700—red; and invisible light range from 100–400—ultraviolet and 700–1400 nm—infrared (WHO, 1979), where 1nm=10^{-9}m]. Planck's law describes the actual intensity distribution as a function of the wavelength, λ, and temperature T as follows:

$$E_\lambda = \frac{C_l}{\lambda^5}\left(e^{C_2/\lambda T}-1\right) \tag{17.18}$$

where E_λ is the energy emitted for a given wavelength or range and C_1 and C_2 are constants. In general, the incoming solar radiations are referred to as short-wave radiations and the spectrum emitted by Earth comprises long-wave radiation. Most of the solar radiation reaching Earth's atmosphere is dissipated before it strikes the soil surface. The dissipation occurs partially as a result of the reflection of radiation by clouds, absorption by water vapor, oxygen, carbon dioxide*, and ozone, and diffusion by molecules and particles in air. Solar radiation reaching Earth's

* Greenhouse gases allow incoming solar radiation to pass through Earth's atmosphere, but prevent most of the outgoing infrared radiation from the surface and lower atmosphere from escaping into outer space. The greenhouse effect is the rise in temperature that Earth experiences because certain gases in the atmosphere (water vapor, carbon dioxide, nitrous oxide, methane, halogenated fluorocarbons, ozone, perfluorinated carbons, and hydrofluorocarbons) trap energy from the Sun. Without these gases, heat would escape back into space and Earth's average temperature would be about 33°C colder. Because of how they warm Earth, these gases are referred to as greenhouse gases (http://www.epa.gov/globalwarming).

surface is partly direct and partly in the form of scattered beams. After striking the crop or canopy, a fraction of incoming radiation is reflected back to the atmosphere, which is known as albedo *(α)*. The thermal radiations are also transmitted from soil surface into the atmosphere Dearth, and onto soil surface from clouds Rsky, therefore net radiation (R_N) is:

$$R_N=(1-a)R_s+R_{nt} \tag{17.19}$$

where R_s is global solar radiation (sum of direct and scattered beam) and R_{nt} is net long-wave thermal radiation $(R_{sky}-R_{earth})$. The R_N varies significantly with climate, latitude, and surface cover. For a known value of emissivity, both R_{sky} and Dearth can be calculated by the Stefan–Bolzmann equation (17.15).

17.9.2 Conduction

Conduction is the primary heat transfer mechanism in soil and refers to the propagation of heat within a soil or another body by molecular motion. It is the transfer of translational, rotational, and vibrational energy from molecule to molecule. The process of heat conduction is analogous to diffusion and both try to equilibrate, or even out, mixer's distribution of molecular kinetic energy. The heat flow by conduction in soil takes place from warmer locations towards the cooler regions. Fourier law explains the heat flow by conduction and macroscopically one-dimensional conduction of heat energy through a soil section is described as follows

$$q_h = -k_T A\left(\frac{\partial T}{\partial z}\right) \qquad (17.20)$$

where q_h is the heat flux (Js^{-1}), k_T is proportionality constant or thermal conductivity ($Jm^{-1}s^{-1}K^{-1}$), A is the area of cross section (m^2), T is the temperature in °K, and $\partial T/\partial z$ is the temperature gradient in degrees per unit length and the slope of the temperature-distance curve. The negative sign in Eq. (17.20) indicates that heat transfer occurs in the direction of decreasing temperature. Thermal conductivity of solids (Table 17.5) varies from 1 J m^{-1} s^{-1} K^{-1} to 100 J m^{-1} s^{-1} K^{-1}. For liquids and gases, it ranges from $0.01Jm^{-1}s^{-1}K^{-1}$ to $1.0Jm^{-1}s^{-1}K^{-1}$ and 0.001 J m^{-1} s^{-1} K^{-1} to 0.1 J m^{-1} s^{-1} K^{-1}, respectively. The ratio of q_h and A is also known as heat flux density ($Jm^{-2}s^{-1}$).

17.9.3 Convection

The transfer of heat energy in a convection process involves the movement of a heat-carrying mass. Infiltration of warm water into an initially cold soil

TABLE 17.5 Thermal Conductivity of Certain Metals (at 25°C)

Metal	Thermal conductivity (cal $cm^{-1}s^{-1}°C^{-1}$)
Aluminium	9.56
Copper	16.25
Gold	2.44
Iron	2.24
Platinum	0.75
Silver	7.05

Tungstun	4.88

Source: Adapted from Handbook of Chemistry and Physics, 1988–89.

results in heat transfer by the process of convection. Newton's first law of cooling can be used to calculate energy fluxes in and out of the system

$$q_v = C_v A v (T_s - T_0) \text{ or } L*E \quad (17.21)$$

where q_v is the heat flux of convection (Js^{-1} or W), C_v is the volumetric heat capacity ($Jm^{-3}K^{-1}$), v is the velocity of fluid (m s^{-1}), T_s is the temperature of the soil in contact with fluid (K), T_0 is the temperature of the fluid far away from the surface (K), L is latent heat of vaporization, and E is evaporation rate. The convection phenomenon is probably more important in the atmosphere, where there is a consistent circulation of warm and cold air and heat exchange. In soils, the heat convection phenomenon is less important in general, however, during infiltration and redistribution of water in the soil profile, which is cooler than the incoming water, convectional heat energy transport becomes important.

17.10 OTHER PROCESSES OF HEAT EVOLUTION AND TEMPERATURE IN SOIL

17.10.1 Condensation

The conversion of water vapor to a liquid state is known as condensation. Condensation is an exothermic process, and the heat energy released in condensation warms the soil surface. A similar phenomenon is observed when liquid water freezes. About 600 cal g^{-1} of heat energy is released when water vapor condenses, whereas 80 cal g^{-1} of heat (of fusion) is taken up when soil freezes. The six-phase changes that water can undergo and the heat gained and lost is given in Table 17.6.

TABLE 17.6 The Six Phase Changes That Water Can Undergo and the Heat Gained and Lost

Process	From	To	Heat gained/lost ($calg^{-1}$)
Condensation	Vapor	Liquid	600
Evaporation	Liquid	Vapor	−600
Freezing	Liquid	Ice	80
Melting	Ice	Liquid	−80
Deposition	Vapor	Ice	680
Sublimation	Ice	Vapor	−680

Source: Modified from http://www.usatoday.com/weather/wlatentl.htm.

17.10.2 Microbial Processes and Heat Evolution

Diverse communities of organisms are present in soil. Variations of microbial population, distribution and activity are a function of depth and type of soil including structure, texture, and water status (Misthustin, 1956). Metabolism is defined as the sum of all chemical reactions occurring within a living organism. Catabolic reactions are exergonic or energy-releasing reactions, which break down more complex molecules, usually by hydrolysis, into simpler components (e.g., chemical processes of digestion). Anabolic reactions are endergonic or energy requiring and build more complex molecules, usually by condensation, from subunit components. The energy for anabolic reactions is provided by catabolic reactions. Microorganisms decompose the organic matter present in the soils and heat energy is released. An example of an exergonic reaction is the fermentation of alcohol as follows:

$$C_6H_{12}O_6 \rightarrow 2C_2H_5OH + 2CO_2 + 226\ kJ \quad (17.22)$$

17.10.3 Chemical Reactions and Heat Evolution

Oxidation and reduction reactions (REDOX reactions) are always coupled in biological systems. Oxidation reactions are exothermic (or exergonic) and release energy, whereas reduction reactions are endothermic (or endergonic) and harness energy. Chemical reactions may be viewed in terms of the amount of energy required by the reaction at various stages. A convenient way to do this is with an energy hill diagram. In these diagrams, the total amount of energy, both kinetic and potential in the chemicals involved in the reaction, is plotted as a function of time. Conversion of sulfur (S) to sulfur dioxide (SO_2) and to sulfuric acid (H_2SO_4) are examples of exothermic processes.

$$S + O_2 \rightarrow S0_2 \quad (17.23)$$

$$2SO_2 + O_2 \rightarrow 2SO_3 \quad (17.24)$$

$$SO_3 + H_2O \rightarrow H_2SO_4 \quad (17.25)$$

The above chemical reaction releases about 178 Kcal/mole of energy (Bohn et al., 1934). Chemical reactions are known as *exothermic* when the chemical products of the reaction have less energy than the starting materials. Another example of an exothermic reaction is burning wood or a burning match. Wood is mainly cellulose and has a lot of chemical energy. The products of burning (e.g., CO_2 and H_2O) have much less energy because the net balance of the energy is converted into light and heat.

Chemical reactions that lead to products having more energy at the end than at the beginning are called *endothermic*. Endothermic reactions typically involve the synthesis of complex molecules from simple ones. Examples of endothermic reactions are cells making proteins from amino acids and photosynthesis in plant cells. In photosynthesis, CO_2 and H_2O, which are the starting materials for photosynthesis, have less energy than

the final product, i.e., carbohydrates (http://old.jccc.net/~pdecell/metabolism/energyhill.html).

17.11 ENERGY BALANCE OF SOIL

Net radiation is the sum of all incoming minus all outgoing radiation on Earth's surface. Steady state one-dimensional heat energy balance at the soil surface or crop canopy can be written as

Net heat energy arriving at surface
− net heat energy leaving surface=0* (17.26)

Equation (17.26) disregards the transient energy changes due to heating or cooling of soil surface and lateral heat energy inputs. Heat transfer

* Except in a greenhouse, where net heat energy leaving the surface is smaller, therefore, Eq. (17.26) is not satisfied.

from the soil surface takes place as (i) convective heat flux (H_c), (ii) soil heat flux (J_H) and (iii) latent heat flux $(L*E)$. H_c represents the transport of warm air from the soil surface to the atmosphere vertically above it. The J_H represents the vertical transport of heat into the soil, and $L*E$ denotes evaporation and subsequent transport of water vapor from the soil surface (L is the latent heat of vaporization and E is the evaporation rate). The net radiation received by the soil surface is transformed into heat, which warms soil and air and vaporizes water. Therefore, under steady state conditions the heat balance equation can be written as

$$R_N=H_c+J_H+L*E \tag{17.27}$$

Combining Eqs. (17.19) and (17.27) provides the total surface energy balance as follows

$$(1-\alpha)Rs+Rnt-(H_c+J_H+L*E)=0 \tag{17.28}$$

17.12 HEAT CAPACITY OF SOIL

The heat capacity of soil as defined in Sec. 17.5.1 is the amount energy required to change the temperature of a body by 1°C by heat adsorption or release. The relationship between volumetric and gravimetric heat capacities for a dry soil is described in Eq. (17.8), which is rewritten below:

$$C_v=\rho_b*C_g \tag{17.8}$$

and for a wet soil

$$C_v = \rho_b' * C_g = \rho_b(1 + w) * C_g = (\rho_b + \theta) * C_g \quad (17.29)$$

where ρ_b' is wet bulk density, w is gravimetric water content, and θ is volumetric water content. The C_v is dependent on composition of solid phase, which constitutes mineral and organic matter, bulk density, and water content of soil. The total C_v is calculated by summing the heat capacities of various constituents, weighted according to their volumes (de Vries, 1975)

$$C_v = \Sigma(f_{si}C_{si} + f_wC_w + f_aC_a) \quad (17.30)$$

TABLE 17.7 Thermal Conductivity and Heat Capacity of Gases (Oxygen at 25°C, 1 atm), Water (26.7°C), Quartz (37.8°C), and Sandstone (100°C)

Gas	Thermal conductivity (k_T) (10^{-6} cal cm^{-1} s^{-1} $°C^{-1}$)	Heat capacity (C_g) (cal $g^{-1}°C^{-1}$)
Air	62.2	0.25
Carbon dioxide	39.67	–
Oxygen	63.64	0.219
Water	42.57	0.998
Quartz (C-axis)	6.4	0.18
Sandstone	3.82	0.26
Iron		

Source: Adapted from Handbook of Chemistry and Physics, 1988–89.

where f is the volumetric fraction of each constituent phase, subscript s, w, a, and f stand for solid, water, air, and number of components in a given phase. The gravimetric heat capacity is the ratio of volumetric heat capacity and particle density (Table 17.7). The heat capacity of loam, sandy loam, sandy clay loam, a clay loam, and clay soil is given in Table 17.8. The heat capacity for each of the components solid, water, and air is the product of their particle density and specific heat or heat capacity per unit mass, i.e., $C_{si}=\rho_{si}C_{mi}$, $C_w=\rho_wC_{mw}$, and $C_a=\rho_aC_{ma}$. In general, the contribution of air is almost negligible because of the very small density and is ignored. The solid phase is divided into two components: mineral (m) and organic matter (o). Eq. (17.30) can be rewritten as

$$C_v = \sum(f_mC_m + f_oC_o + f_WC_W) + f_oC_o + f_wC_w) \quad (17.31)$$

17.13 THERMAL CONDUCTIVITY

The thermal conductivity *(k_T)* is defined as the quantity of heat transferred through a unit cross-sectional area in unit time under a unit temperature gradient. The K_T of soil depends upon the volumetric proportions of the solid, liquid, and gaseous phase of the soil medium. The other factors, which influence K_T, are the size and arrangement of solid particles, and interfacial contact between solid and liquid phases. The K_T values of some materials is presented in Tables 17.7 and 17.9, which show that air has a much lower K_T than water and solid, therefore, high air content reduces the thermal contact between soil

TABLE 17.8 Heat Capacity of Some Nigerian Soils

Soil texture	Heat capacity ($calg^{-1}\,°C^{-1}$)
Sandy loam	0.322
Sandy clay loam	0.350
Loam	0.279
Clay loam	0.224
Clay	0.248

Source: Modified from Ghuman and Lal, 1985.

TABLE 17.9 Range and Averages of Thermal Diffusivity and Thermal Conductivity of Soil Particles

		Thermal diffusivity $\times 10^{-3}$ (cm^2s^{-1})		Thermal conductivity $\times 10^{-3}$ ($calcm^{-1}s^{-1}°C^{-1}$)	
Soil type	Moisture state	Range	Average	Range	Average
Sand	Dry	3.5–1.5	2.23	0.55–0.37	0.42
	Wet	12.6–4.4	8.0	4.35–3.7	4.02
Clay	Dry	1.8–1.2	1.5	0.37–0.17	0.26
	Wet	11–3.2	5.97	3.5–1.4	2.69

Source: From Geiger, 1965; Nakshabandi and Kohnke, 1965; and van Duin, 1963.

particles and reduces the K_T of soil. On the other hand, an increase in bulk density of soil lowers the porosity and improves the thermal contact between soil particles and increases K_T and D_T (cm^2s^{-1}). The increase in water content of the soil also improves the thermal contact between soil particles and increases K_T as well as D_T.